Electrons in coupled stereo-irregular chains

S. Stafström, R. Riklund, and K. A. Chao
Department of Physics and Measurement Technology, University of Linköping, S581 83 Linköping, Sweden
(Received 3 May 1982; revised manuscript received 2 December 1982)

Two interacting stereo-irregular chains of hydrogen atoms coupled at a finite number of bridge points are simulated by a computer and are solved numerically via the unrestricted Hartree-Fock approximation with a modified spin-polarized potential. The electron localization is studied with the inverse participation ratio and the moment analysis. We discovered that the eigenstates in the lower part of the spectrum are localized around the bridge points due to the random ionic potential. The resultant random potential is screened by the electrons occupying the intermediate region of the spectrum. Thus electrons near the Fermi energy feel a smooth potential and can tunnel through the bridge points. Connection between the present calculation and conducting polymers is discussed.

I. INTRODUCTION

In order to obtain reliable quantitative results for understanding the electronic properties in disordered systems, recently there have been many numerical investigations. Most of the calculations are based on the tight-binding Anderson Hamiltonian[1] with various computation schemes.[2–14] Besides its intrinsic theoretical interest, the problem of electronic properties in one-dimensional random systems has been extensively studied in connection with the quasi-one-dimensional materials such as the charge-transfer salts and the conducting polymers. The recent review by Andre[15] summarizes the numerical studies of realistic chain systems with the Hartree-Fock,[16–20] the self-consistent-field–linear combination of atomic orbitals,[21–25] the extended–Hückel-theory,[26–28] the crystal-orbital,[29] the coherent-potential approximation[30] (CPA), and the band-structure calculation[31] methods.

It is desirable to calculate all the interaction strengths in a model with a set of atomic wave functions, instead of treating them as adjustable parameters. Such first-principle calculation is certainly very difficult, and so far only a periodic straight chain of hydrogen atoms has been thoroughly analyzed.[32–28] To incorporate such a type of calculation in disordered systems, we have performed an unrestricted Hartree-Fock calculation with a modification of the spin-polarized potential, assuming a stereo-irregular chain structure of hydrogen atoms.[39]

Although many authors have attempted to interpret the physical properties of quasi-one-dimensional materials with the model of a single chain, the neglect of the coupling between chains is a serious drawback. For example, it is generally accepted that the structure of many conducting polymers can be viewed as intermingled fibrils of finite length. Without the coupling between fibrils, each electron is restricted to a single isolated fibril and so cannot conduct current. Regardless of its relevance to conducting polymers the coupling between chains is an interesting problem not much studied yet.[40,41]

In this paper we will investigate numerically the electronic properties in two coupled stereo-irregular chains. We are particularly interested in the case in which the two chains are strongly coupled at a finite number of bridge points. This kind of topological structure can be easily generated with a computer as will be illustrated in Sec. II. In order to investigate the electron localization, we must first derive an effective one-electron Schrödinger equation from the complete many-electron Hamiltonian. In Sec. III we outline the computation scheme of the unrestricted Hartree-Fock approximation with a modified spin-polarized potential. The effect of disorder on the single-particle density of states (DOS) can then be readily demonstrated. The inverse participation ratio has been used by many authors[6,9,14,42,43] to measure the degree of localization. In Sec. IV we calculate both the inverse participation ratios and the moments of all the eigenstates to check their degrees of localization. The interesting phenomena of electron localization and electron tunneling around the bridge points will be discussed in Sec. V. In Sec. VI we close this paper with a short remark on the relevance of the present calculation to the conducting polymers.

II. TOPOLOGICAL STRUCTURE

Figure 1 shows the topological structure of two coupled stereo-irregular chains generated by computer. We consider the upper-half space ($Z \geq 0$) of a

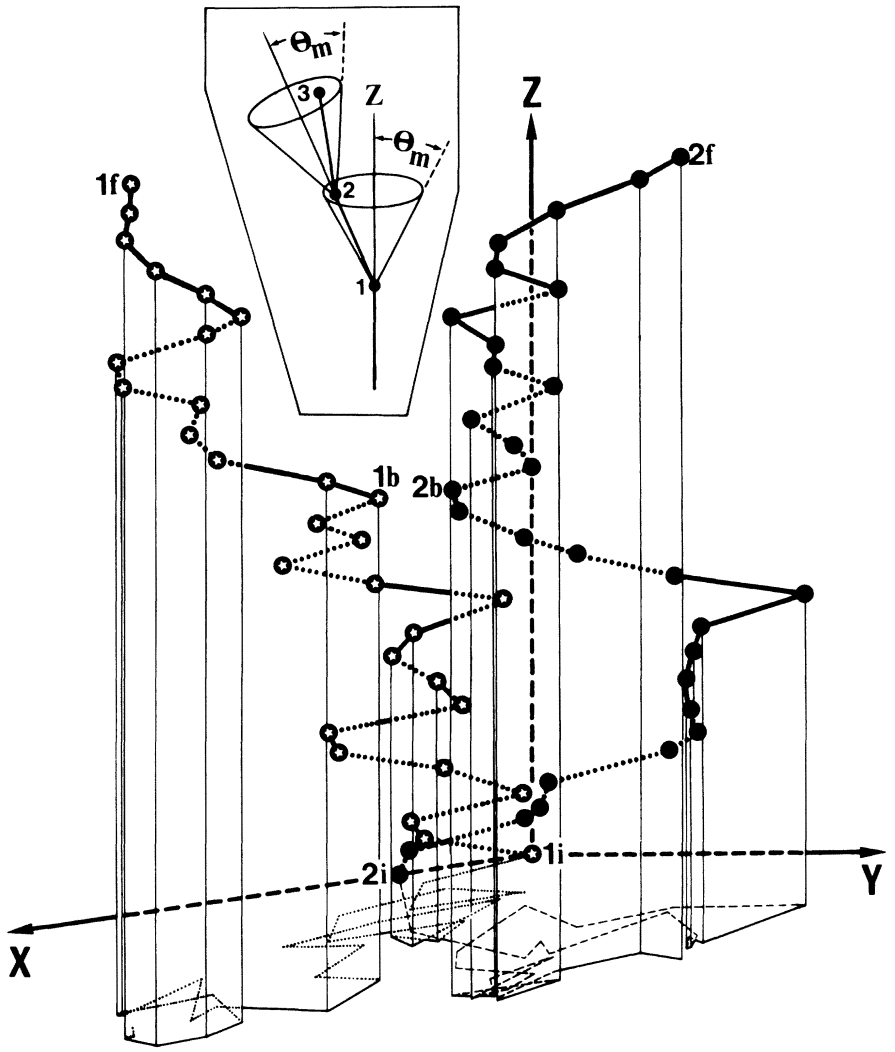

FIG. 1. The structure of two stereo-irregular chains 1i-1b-1f and 2i-2b-2f generated by a computer. Atoms 1b and 2b form the bridge point. The scales along the three axes are different, but all the bondlengths have constant value R_0. Point 2i is on the X axis with a distance D from the origin 1i.

Cartesian coordiate system (X,Y,Z) with one atom at the origin (the atom 1i in Fig. 1, or the atom 1 in the inset of Fig. 1). Taking the Z axis as the symmetry axis, we construct a right circular cone of angle θ_m with its tip at the origin. A point in the cone with a distance R_0 from the origin (point 2 in the inset in Fig. 1) is picked randomly by the computer, marking the position of atom 2. Then we choose the line from atom 1 to atom 2 as the symmetry axis of the second cone, as illustrated by the inset in Fig. 1. The position of atom 3 with a distance R_0 from atom 2 is again chosen randomly in the new cone by a computer. The process repeats itself until the first stereo-irregular chain of N_1 atoms is generated. The topological structure of this chain is given in Fig. 1 as the star chain 1i-1b-1f. Next, we put one atom at the position 2i on the X axis, with a distance D from the origin, as the starting first atom, to generate the second stereo-irregular chain of N_2 atoms (the dot-chain 2i-2b-2f). This process of chain generation is exactly the same as the one used in Ref. 39 (referred to as I). Therefore, each chain maintains the quasi-one-dimensional feature along the Z axis even for θ_m as large as $\pi/6$, as was explained in I.

Each stereo-irregular chain is characterized by the constant bondlength R_0 and a set of random bond angles within the range $(\pi-\theta_m,\pi)$. In a system of randomly located stereo-irregular chains, two chains may cross each other with a sufficiently close distance. That is, an atom on one chain is very near to an atom on the other chain. For convenience, we call the small region surrounding these atoms a

"bridge point." The bridge points represent the most important coupling in a random system of coupled chains. If the density of the chains is low and θ_m is not very large, along each chain (of finite length) there is only a finite number of bridge points, and two consecutive bridge points are separated by a large number of bondlengths. In other words, the correlation between two bridge points can be neglected. Under the condition of low chain density, the coupling of more than two chains at a single bridge point is also unlikely to occur.

To investigate the physical properties of two coupled stereo-irregular chains, when we generate the second chain the position of the first atom (point 2i) and the symmetry axis of the first cone should be arbitrarily chosen. A large number of such coupled chains must be examined and the results are then configurationally averaged. This kind of calculation is extremely tedious, but can be avoided in the present work where the density of the chains is assumed to be low. Chains are coupled mainly through the bridge points the correlation between which has been neglected. Since the parts of one chain away from the bridge points are not much affected by the other chain, the characteristic feature of the coupled chains does not depend crucially on the relative orientation of those weakly interacting parts of the chains. To study the coupling between chains pairwise is then a reasonable starting point for the general understanding of a system of random chains at low density. Therefore, the initial position (point 2i) and the orientation of the first cone axis have negligible influence of the final results, provided the distance D (between the points 1i and 2i) is much larger than the Bohr radius. Our choice of the starting condition to generate the second chain is for convenience only. Almost all the coupled chains we have generated with $N_1=N_2=30$ and $\theta_m=\pi/6$ come close to each other at bridge points separated by more than 10 bondlengths. Using the structure in Fig. 1 as an example, there are two bridge points. The first bridge point connects atom pair no. 3 and the second bridge point connects atom pair no. 17 (marked as 1b and 2b). If we take $R_0=5$ (in this paper the unit of length is Bohr radius), then the distances between the two atoms in the atom pair no. 3 (R3) and in the atom pair no. 17 (R17) are $(D;\mathrm{R3};\mathrm{R17})=(5;0.5751R_0;0.3744R_0)$, $(6;0.5863R_0;0.3451R_0)$, $(7;0.6611R_0;0.4219R_0)$, $(8;0.7812R_0;0.5629R_0)$, $(9;0.9293R_0;0.7320R_0)$. Since we assume low concentration of chains, for the calculation in this paper we always set $D\geq R_0$.

The first bridge point at the atom pair no. 3 may be introduced artificially due to the choice of the starting condition in generating the second chain. However, the two bridge points are separated by 14 bondlengths. Consequently, our way of generating the chains does not introduce the correlation between the bridge points. The numerical solutions to be presented later indeed justify this simplification. Therefore, the presence of the first bridge point will not affect the main conclusion derived from the present calculation. There are two advantages to generating the coupled chains as we have done. First, if we set $\theta_m=0$ and then $\theta_m\neq 0$, we can easily compare the results of the two cases to examine the disorder effect. Second, by increasing the value of D step by step, we can investigate systematically the effect of the chain coupling on the electronic properties. Nevertheless, we should point out that the physical significance is not associated with the value of D, but to the values of R3 and R17, as well as to the topological structure of the whole system. We can choose the position of point 2i and the first cone axis arbitrarily, and this essentially leads to the appearance of the bridge point somewhere along the chain, provided the chain is long enough. Our choice of the initial condition for generating the second chain is for convenience only, since in this way bridge points appear in coupled chains which are not too long to be solved numerically with a modern computer. Consequently, in the rest of this paper, the statement "dependence of D" actually refers to the dependence of the topological structure of the coupled chains in general, and on the local environments around the bridge points in particular.

III. UNRESTRICTED HARTREE-FOCK DENSITY OF STATES

In order to obtain numerical results, we consider two chains of equal number of *hydrogen atoms*, $N_1=N_2=N/2=30$. The system is electrically neutral. The cone angle is set to be $\theta_m=\pi/6$ or $\theta_m=0$. Throughout the rest of the paper the name *stereo-irregular chain* is for $\theta_m=\pi/6$, and the name *straight chain* is for $\theta_m=0$. The Hamiltonian of the coupled chains is

$$H=\sum_i p_i^2/2m+\sum_i V^{\mathrm{ion}}(\vec{r}_i)+\frac{1}{2}\sum_{i,j}V^{ee}(\vec{r}_i-\vec{r}_j)\,, \tag{1}$$

where $V^{\mathrm{ion}}(\vec{r}_i)$ is the total ionic potential for the ith electron. The Coulomb interaction between the ith and the jth electrons is $V^{ee}(\vec{r}_i-\vec{r}_j)$, and the summations are over all the N electrons. In I (Ref. 39) we solved the same Hamiltonian of a single stereo-irregular chain with the unrestricted Hartree-Fock approximation but the spin-polarized potential is

modified. In this paper the same approach will be used. Let

$$\phi_i(\vec{r}) \equiv \phi(\vec{r}-\vec{R}_i)$$

be the hydrogen 1s wave function centered at the ith atom, and the single-particle eigenfunction of the unrestricted Hartree-Fock equation be constructed as

$$\Psi_{i\sigma}(\vec{r}) = \sum_j \phi_j(\vec{r}) B_{\sigma ij} \ . \tag{2}$$

for the σ spin, then the unrestricted Hartree-Fock approximation leads to two coupled equations for both spin $\sigma=\uparrow$ and $\sigma=\downarrow$,

$$\tilde{B}_\sigma^\dagger \tilde{H}_{0\sigma} \tilde{B}_\sigma = \tilde{E}_\sigma \ . \tag{3}$$

In the above equation $\tilde{B}_\sigma$ is the matrix of the coefficients $B_{\sigma ji}$ and $\tilde{E}_\sigma$ is the diagonal Hartree-Fock eigenenergy matrix for the spin σ.

At the atomic limit, within the manifold of the 1s state, each hydrogen atom can be either neutral with the one-electron energy level E^0, or negatively charged with the two-electron energy level E^-. The strong electron correlation effect must be taken into account in order to obtain the bound state with energy E^- in a negatively charged hydrogen. Chandrasekhar[44] has proposed a two-particle wave function for this bound state, which yields a very accurate binding energy as compared to the observed value. Therefore, the spin-polarized potential included in $\tilde{H}_{0\sigma}$ should be modified wherever two electrons of opposite spins occupy the same atom. The exact form of $\tilde{H}_{0\sigma}$ is very complicated, and can be found in an earlier paper.[45] Of course, $\tilde{H}_{0\sigma}$ de-

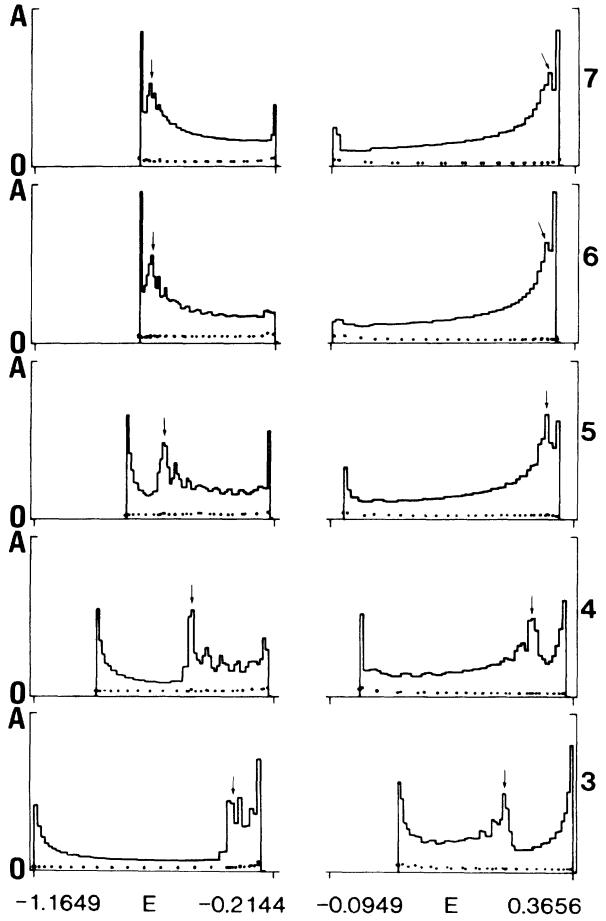

FIG. 2. The density of states (DOS) (histograms) and the IPR (dots) for coupled straight chains with $R_0=3$. The values of D are given on the right-hand side. The unit of energy is the hartree. The value of A is 1 for IPR, 4 for DOS on the left, and 6 for DOS on the right.

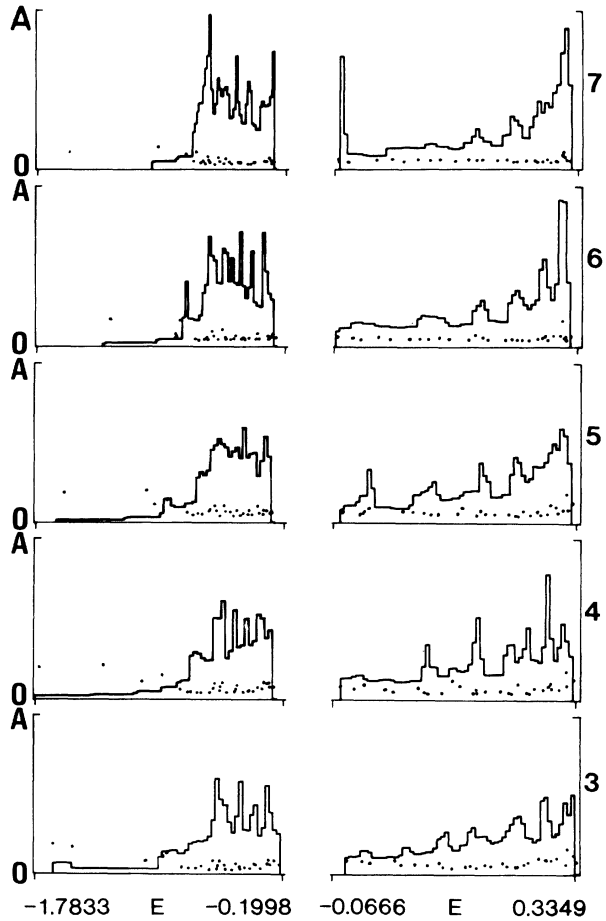

FIG. 3. The density of states (histograms) and the IPR (dots) for coupled stereo-irregular chains with $R_0=3$. The values of D are given on the right-hand side. The unit of energy is the hartree. The value of A is 1 for IPR, 2 for DOS on the left, and 6 for DOS on the right.

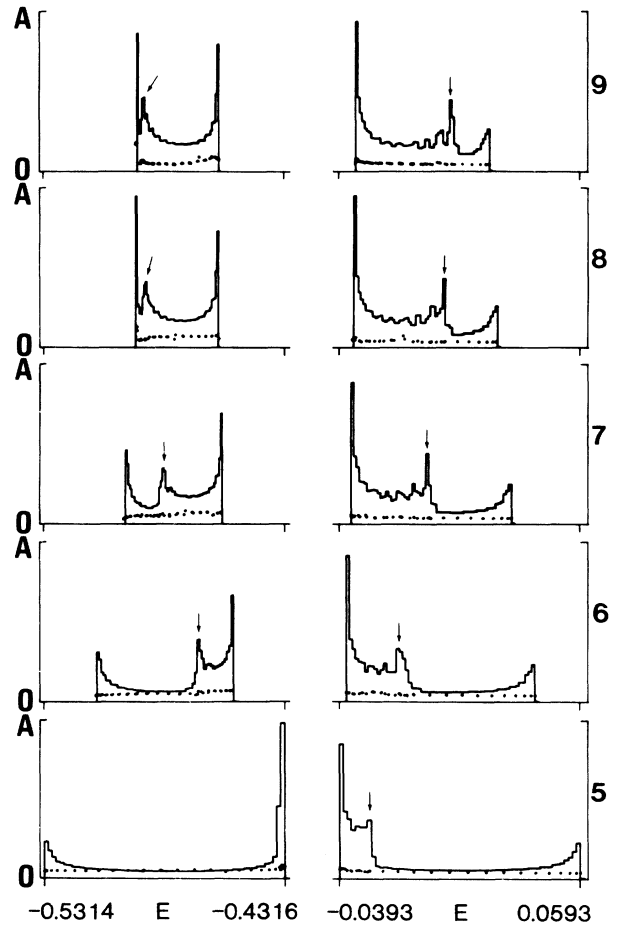

FIG. 4. Same as in Fig. 2 but with $R_0=5$, $A=60$ for DOS on the left, and $A=45$ for DOS on the right.

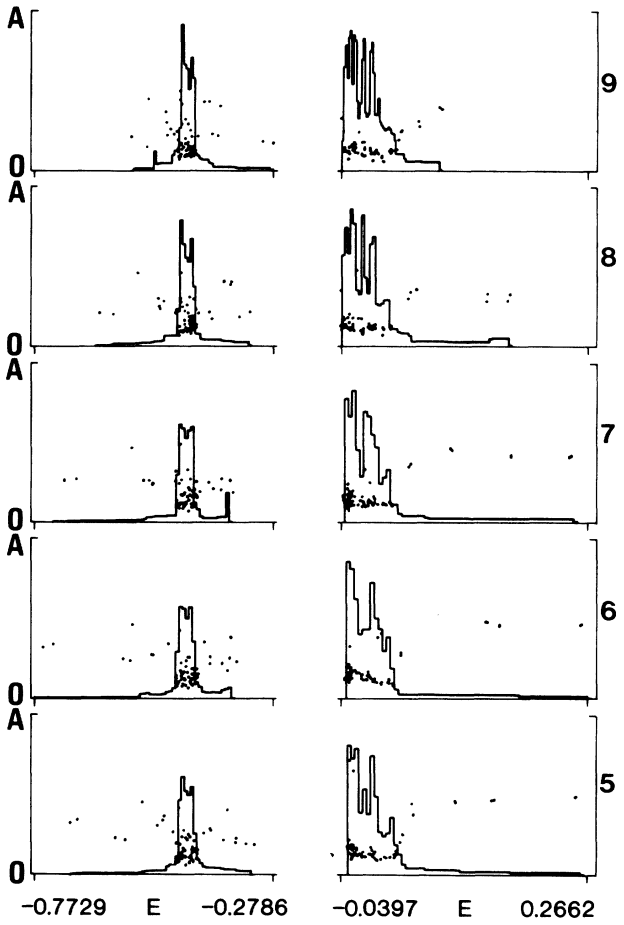

FIG. 5. Same as in Fig. 3 but with $R_0=5$, $A=18$ for DOS on the left, and $A=14$ for DOS on the right.

pends on the number of up-spin and down-spin electrons. In our model it is very unlikely that the ferromagnetic phase is stable. Hence, in our numerical calculation we consider the case of 30 up-spin and 30 down-spin electrons.

For given topological structure of the coupled chains, (3) is solved numerically. The density of state is shown in Fig. 2 for the straight chain with $R_0=3$, in Fig. 3 for the stereo-irregular chain with $R_0=3$, in Fig. 4 for the straight chain with $R_0=5$, in Fig. 5 for the stereo-irregular chain with $R_0=5$, in Fig. 6 for the straight chain with $R_0=7$, and in Fig. 7 for the stereo-irregular chain with $R_0=7$. Owing to the strong intra-atomic correlation, each spectrum is split into a lower and an upper subspectrum. In each figure, the left column represents the density of states of the lower subspectrum and the right column represents that of the upper one. The number on the right-hand side of each figure marks the corresponding value of D.

Let us first examine Fig. 2. All histograms show the general structure with three peaks. With increasing D the position of the middle peak (indicated by an arrow) moves toward outside edge of the corresponding density of states. When D becomes very large, the two straight chains are no longer coupled and the density of state is then identical to that of a single straight chain. In fact, when $D/R_0=\frac{7}{3}$ the situation is already very close to the limiting uncoupled chains. It is well known that for a single straight chain the density of states for each subspectrum is a smooth curve with only two peaks at the edges. It is interesting to note that in each column the position of the midpoint between the middle peak and the outside-edge peak is almost the same for all values of D, and almost coincides with the outside-edge-peak position of the corresponding subspectrum of the limiting uncoupled chains. Therefore, the sequence of histograms in Fig. 2 suggests that the coupling between the two chains splits the outside edge of each subspectrum.

If we compare Figs. 2, 4, and 6, we see that the *strength* of the split increases with R_0. At the limit of strong split, the middle peak and the inside-edge peak merge into one, as can be seen in Figs. 4 and 6. The variation of the *strength* of the split with R_0 is

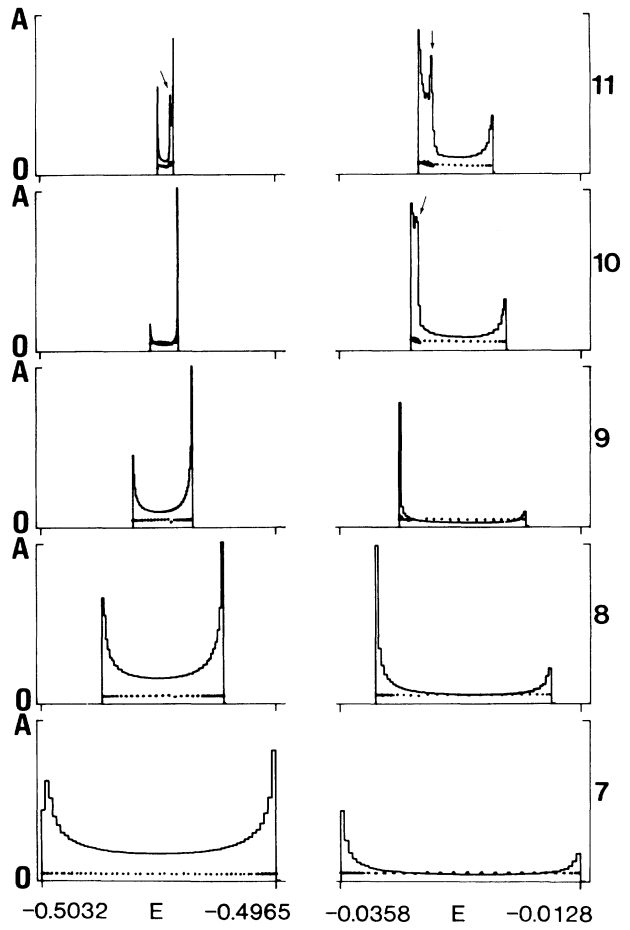

FIG. 6. Same as in Fig. 2 but with $R=7$, $A=300$ for DOS on the left with $D=7$, $A=600$ for DOS on the left with $D=8$, $A=1800$ for DOS on the left with $D=9$, $A=9000$ for DOS on the left with $D=10$, $A=6000$ for DOS on the left with $D=11$, $A=300$ for DOS on the right with $D=7$, 8, 10, and 11, and $A=600$ for DOS on the right with $D=9$.

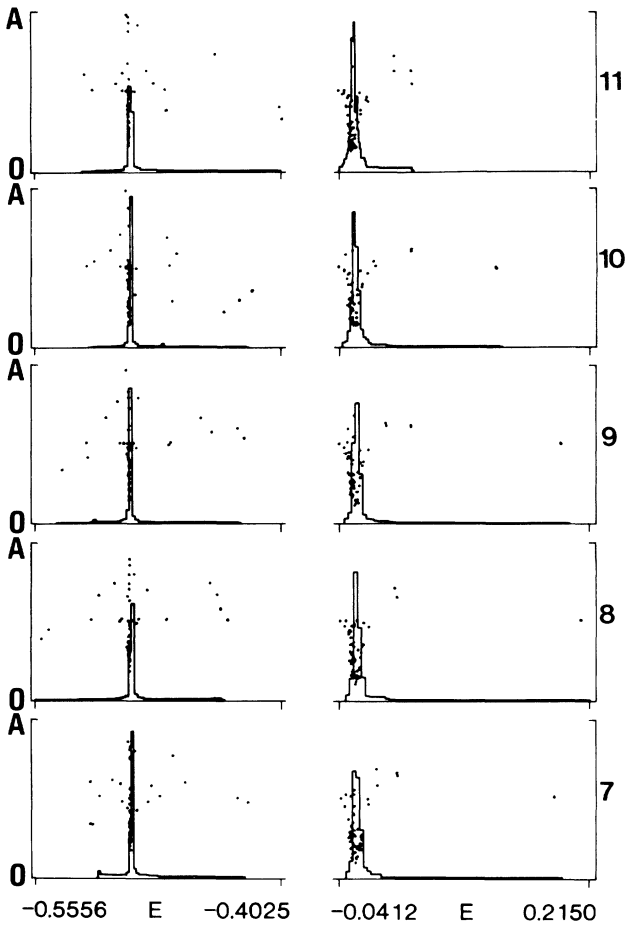

FIG. 7. Same as in Fig. 3 but with $R_0=7$, $A=200$ for DOS on the left, and $A=65$ for DOS on the right.

related to the antiferromagnetic ordering. It has been shown in I that a single straight chain is antiferromagnetically ordered for large R_0. If $D \geq R_0$, two antiferromagnetic chains are again coupled antiferromagnetically. We should point out that here the *strength* of split is measured relative to the width of the subspectrum. The actual *amount* of split depends on R_0 and D in a complicated way; note that the energy scales in Figs. 2, 4, and 6 are different.

Next, we examine Fig. 3 for the coupled stereo-irregular chains with $R_0=3$. The long tails in the density of states are due to the localized states around the bridge point, as will be seen in Sec. V. Besides these long tails all the density-of-states histograms have rather sharp edges. This is the same feature appearing in the density of states of a single stereo-irregular chain.[39] Therefore, the intrachain coupling is much stronger than the interchain coupling to prevent the disorder from having three-dimensional character. When R_0 increases, we see, in Figs. 5 and 7, that the density of states approaches the typical shape for three-dimensional disorder systems. Figures 3, 5, and 7 can be interpreted as follows. For a single stereo-irregular chain, due to the constant bondlength, the dominating disorder effect comes from the randomness in second-neighbor interaction. It has been clearly demonstrated in I that such a physical disorder effect is rather weak even though the topological disorder may be very strong, except for large R_0 accompanied with antiferromagnetic ordering. Let ξ be the characteristic interaction length in our system. If ξ is much larger than R_0, then within a sphere of radius ξ centered at any atom, two chains can still be recognized. Only when R_0 is comparable to ξ does the distribution of atoms within this sphere show three-dimensional disorder. This explanation manifests itself in the next section when we investigate the electron localization.

IV. ELECTRON LOCALIZATION

Let us first check the localization of the single-particle eigenstate (2) via the inverse participation ratio (IPR) defined as

$$\mathscr{R}_{\sigma i}=\left[\sum_j |B_{\sigma ji}|^4\right]\Big/\left[\sum_j |B_{\sigma ji}|^2\right]^2 . \tag{4}$$

For an infinite system with an orthonormal basis, the value of IPR varies from zero for extremely extended states to one for extremely localized states. Although these two conditions are not satisfied for exact numerical solutions in a finite system, IPR has been used by many authors to estimate the degree of localization of eigenstates in a finite system.

In Figs. 2–7 the plottings of the $\mathscr{R}_{\sigma i}$'s versus the eigenenergies are shown by the dots. The vertical scale for IPR in all cases are the same with $A=1$. From Figs. 2, 4, and 6 it is obvious that all the single-particle eigenstates are extended states. Although the values of the IPR in Fig. 3 are larger than those in Fig. 2, none of them is large enough to suggest the existence of a well-localized state. This type of behavior is very similar to that observed in a single stereo-irregular chain with $R_0=3$.[39] Consequently, we conclude *from the IPR analysis* that for $R_0=3$ the random coupling between the two stereo-irregular chains only very weakly localizes extremely few states.

When R_0 increases to 5 and 7, Figs. 5 and 7 indicate the stronger and stronger localization of the eigenstates in the band tails. It was demonstrated in I that for larger R_0, the eigenstates are sublattice Bloch states with antiferromagnetic ordering. The disorder energies in both the intrachain and interchain couplings are of the same order as the antiferromagnetic coupling strength. Therefore, for large R_0 the randomness in two coupled stereo-irregular chains has the three-dimensional feature. This clarifies the discussion at the end of the previous section.

To investigate the electron localization in more details, we have calculated the second moments:

$$L^z_{i\sigma}=\frac{1}{Z}\langle\Psi_{i\sigma}(\vec{r})\,|\,(z-\langle z\rangle)^2\,|\,\Psi_{i\sigma}(\vec{r})\rangle^{1/2} , \tag{5}$$

$$L^y_{i\sigma}=\langle\Psi_{i\sigma}(\vec{r})\,|\,(y-\langle y\rangle)^2\,|\,\Psi_{i\sigma}(\vec{r})\rangle^{1/2} , \tag{6}$$

and

$$L^x_{i\sigma}=\frac{1}{D}\langle\Psi_{i\sigma}(\vec{r})\,|\,(x-\langle x\rangle)^2\,|\,\Psi_{i\sigma}(\vec{r})\rangle^{1/2} , \tag{7}$$

of the σi eigenstate, where Z is the longer one of the projected lengths of the two chains along the Z axis. The y moment $L^y_{i\sigma}$ is not normalized, so it also measures directly the departure of the stereo-irregular chains from the XZ plane. The up-spin moments are plotted in Figs. 8–10 for $R_0=3$, 5, and 7, respectively. In all these figures solid curves are for the coupled straight chains while the dots are for the coupled stereo-irregular chains. The horizontal axis labels the eigenstates with increasing eigenenergy. We should remind the reader that only the lower half of the eigenstates are occupied. For compar-

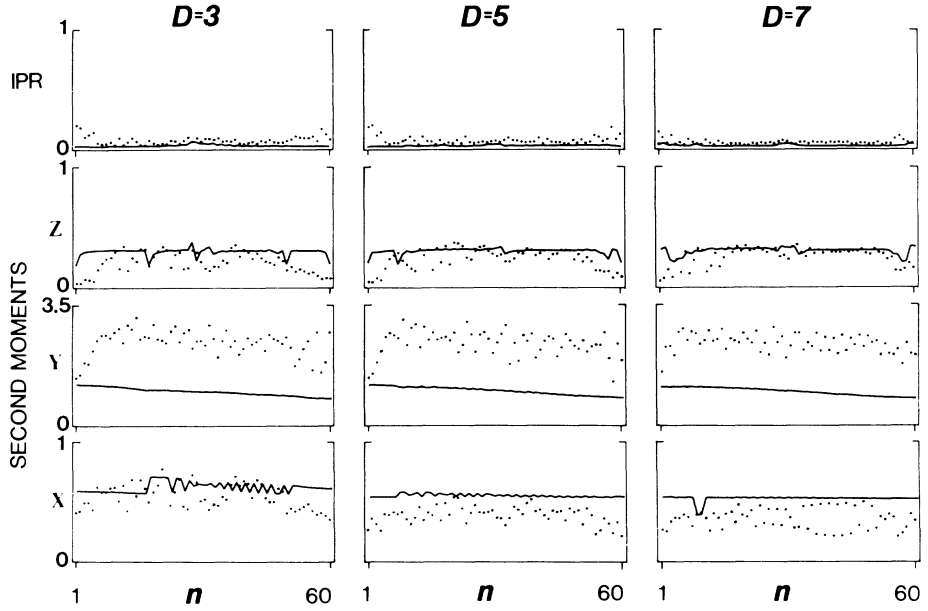

FIG. 8. IPR and moments for up-spin eigenstates with $R_0=3$. Solid curves are for coupled straight chains and dots are for coupled stereo-irregular chains. The eigenstate index n is numerated with increasing eigenenergy.

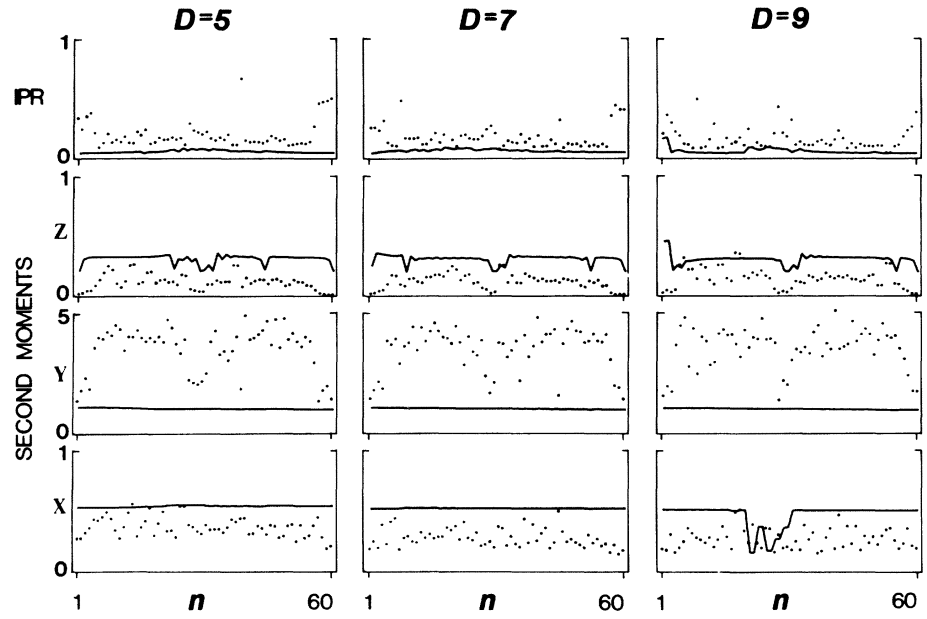

FIG. 9. Same as in Fig. 8 but with $R_0=5$.

ison, the IPR data are also included.

For the case of straight chains, all the moments behave normally in accordance with the delocalized wave functions along the chains. The coupling between the chains is reflected by the x moment having a value around 0.5. The value of the y moment lies around 1, which is the limiting value of an isolated hydrogen $1s$ wave function. The fluctuation of the moments is due to the detailed balance between various contributions to the total energy in reaching the self-consistent solution.

When the coupled chains turn into stereo-irregular structure, the z and the x moments are reduced as a result of both the intrachain and interchain electron localizations. The increase of the y moment is caused by the deviation of the structure from a planar type. We should point out that the first 30 eigenstates ($1 \leq n \leq 30$) belong to the lower subspectrum and the last 30 eigenstates ($31 \leq n \leq 60$) belong to the higher subspectrum. Between them there is an energy gap. From the behavior of the moments, we see that with increasing value of R_0,

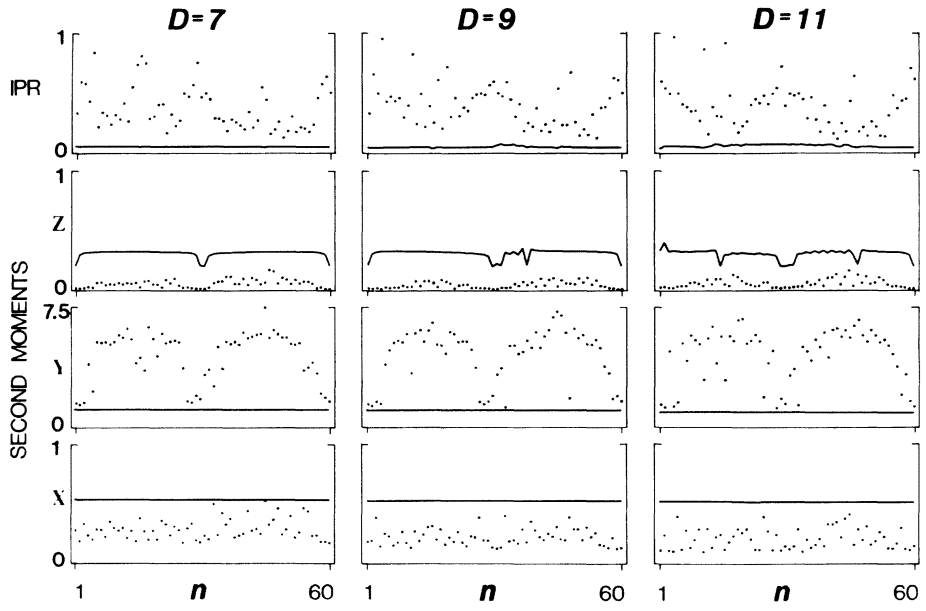

FIG. 10. Same as in Fig. 8 but with $R_0=7$.

the states near the outside edges of the subspectra (near $n=1$ and $n=60$) start to localize first, then the states near the inside edges of the subspectra also become localized, and finally all the states in the whole subspectra are localized. It is important to notice that for $R_0=3$ strongly localized states lie only near the outside edges of the subspectra. We will return to this point when we study the tunneling phenomena around the bridge point. If we compare the z moments in Figs. 8–10 with the corresponding second moments in I for a single stereo-irregular chain, we see a larger fluctuation in the present result. This is because of the existence of the bridge point, and is again related to the tunneling phenomena to be discussed later. The fluctuations in the x and y momenta have their origin in the variation of the interchain distance.

Finally, let us compare the IPR data and the moments, especially the z moment. For example, we examine Fig. 8. Many states should be delocalized according to the IPR criterion, but are largely localized according to the moment analysis. This difference, however, suggests that the moment analysis gives the precursor to effects which occur near the mobility edge at small length scales.

V. ELECTRON TUNNELING AROUND THE BRIDGE POINT

Because the two stereo-irregular chains are coupled through a finite number of bridge points, it is possible to have an eigenstate extended over part of one chain and part of the other chain, with the two parts linked at one or more bridge points. This kind of localization (or delocalization) is difficult to identify even with the moment analysis. In this section, we will investigate in more detail the properties of the eigenstates.

Let us define a path starting from the end point 1i of the first chain in Fig. 1. The path traces along the first chain 1i-1b-1f. Similarly, we define another path 2i-2b-2f along the second chain. The total length of each path is $29R_0$. Then, we calculate the electron density $|\Psi_{i\sigma}(r)|^2$ along these paths. The presentation of $|\Psi_{i\sigma}(r)|^2$ as a function of r is illustrated in Fig. 11 at the bottom of the right side. Along the horizontal axis r starts from the first atom (marked point 1) of the first chain, moves to the last atom of the first chain (marked point $30R_0$), then starts again from the first atom (marked point 1) of the second chain, and finally ends at the last

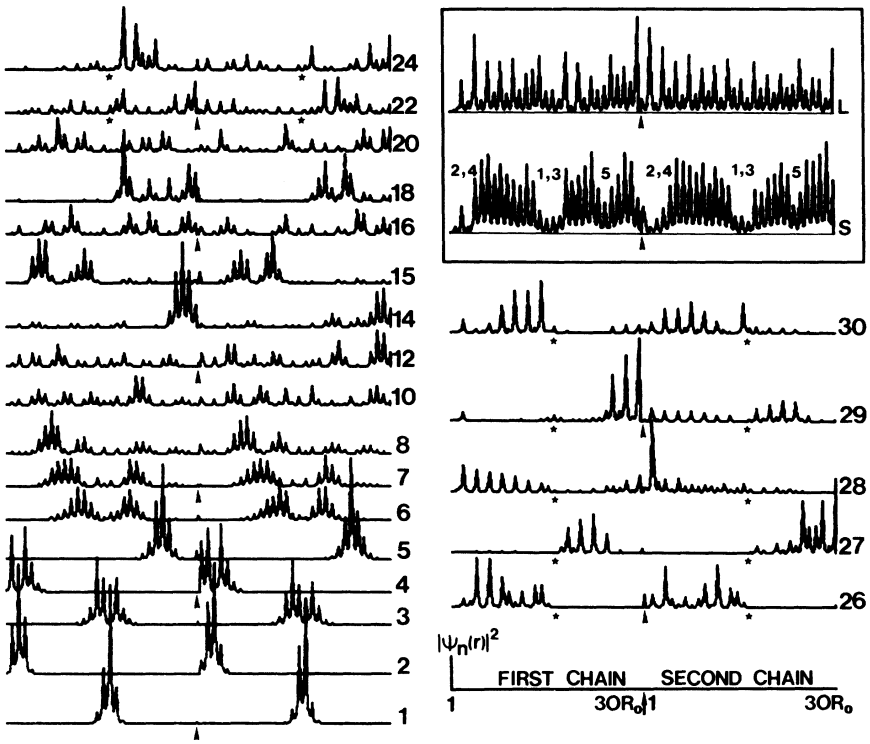

FIG. 11. The charge distribution along the coupled chains for various occupied eigenstates indicated by the number at the right end. Inset shows the averaged charge distribution over the screening region (S), and over the linking region (L). The parameters are $\sigma=\uparrow$, $R_0=3$, and $D=3$.

atom of the second chain (marked point $30R_0$). For $\sigma=\uparrow$, $R_0=3$ and $D=3$, the electron density $|\Psi_{i\uparrow}(r)|^2$ is plotted in Fig. 11 with the values of i indicated at the right side. i is numerated with increasing eigenenergy. Since only 30 states are occupied for each spin, we have ignored all the empty states. In each plot the two chains are separated by an arrowhead, and the bridge point (1b, 2b) is marked by two stars.

The five lowest energy states are extremely localized. There are three bridge points in this system of coupled stereo-irregular chains. The ground state is localized around the narrowest bridge positioned at the bridge point (1b,2b). The $i=2$ state localizes around another bridge point near the end (1i,2i), and the $i=5$ state is localized around the third bridge point near the other end (1f,2f). Strictly speaking, the third bridge point is only vaguely defined since around this point the separation between the two chains is rather large. The electron localization around this point is mainly due to the electron correlation effect. There is almost no overlap between these three localized states. Hence, these bridge points are not correlated as we have mentioned at the end of Sec. II. If we reexamine Fig. 8, we see that the localization of these states is unambiguously indicated by the moments, but not by the IPR.

Now let us average $|\Psi_{i\uparrow}(r)|^2$ over the states from $i=8$ to $i=20$. The result is plotted at the bottom of the inset (marked as S) in Fig. 11. The positions of the empty voids coincide with the positions of five localized states $i=1$, 2, 3, 4, and 5. Therefore, the potential produced by the five electrons trapped at the bridge points is screened by those electrons occupying the states $i=8, 9, \ldots, 20$. The rest of the electrons which occupy the states near the Fermi energy ($i\geq 21$) feel a screened smooth potential, and so are delocalized. If we further average $|\Psi_{i\uparrow}(r)|^2$ over the states from $i=21$ to $i=30$, the result is shown at the top of the inset (marked as L) in Fig. 11. This average charge density indeed extends over the whole system. Consequently, the entire low subspectrum can be divided into three regions; the states in the low-energy region are localized due to the random ionic potential, the electrons occupying the states in the intermediate-energy region provide the main screening strength, and all the states in the high-energy region are extended.

A careful examination of these extended states reveal their special feature as tunneling states. Take the state $i=28$ as an example. We can imagine that one electron moves along the first chain from the end point 1i toward the point 1b (marked by a star), tunnels through the bridge point to the point 2b (also marked by a star) on the second chain, and

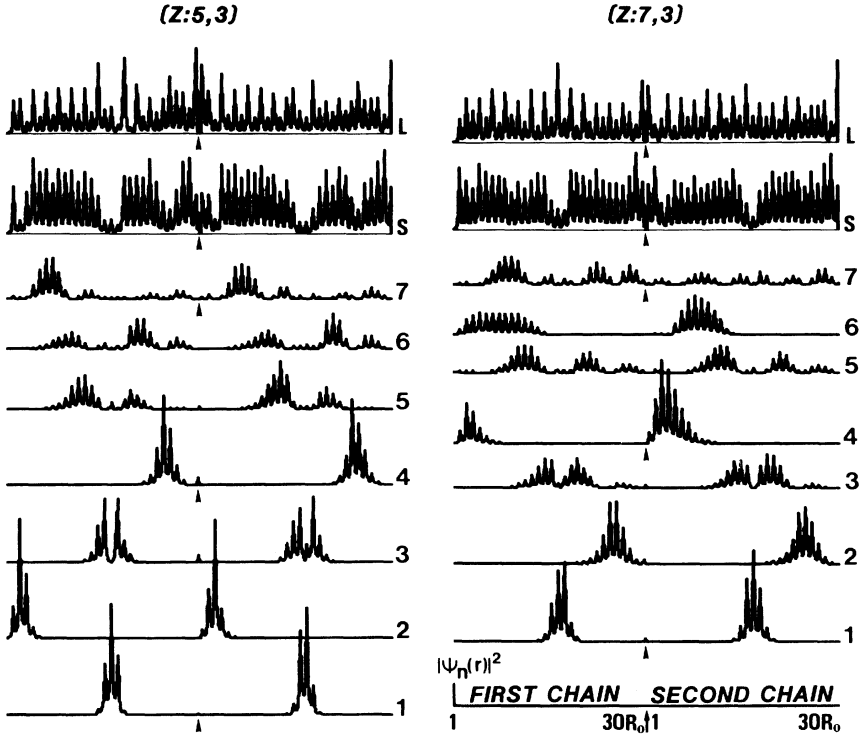

FIG. 12. Same as in Fig. 11 but with $D=5$ (left part) and $D=7$ (right part).

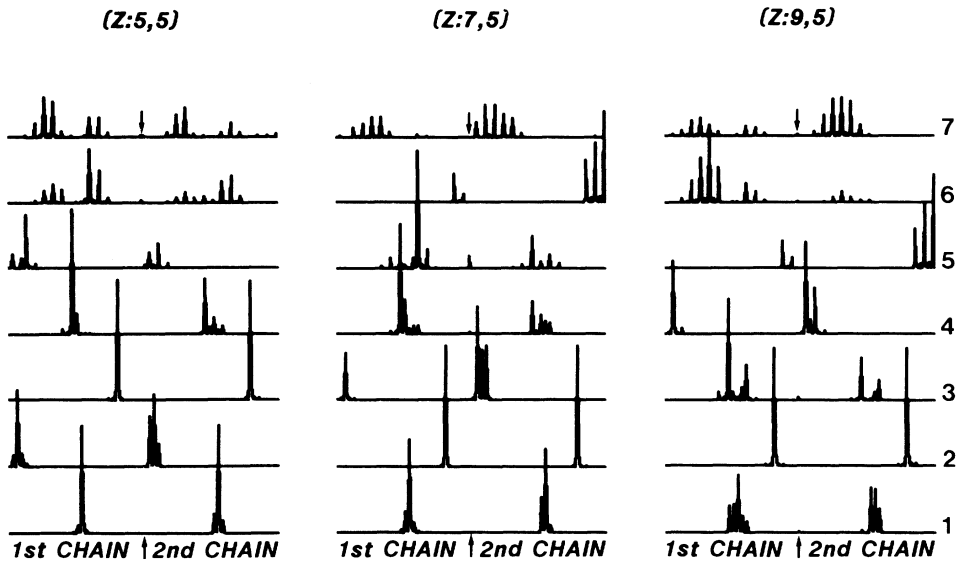

FIG. 13. The charge distribution along the coupled chains for $\sigma=\uparrow$, $R_0=5$, and $D=5$ (left part), $D=7$ (middle part), and $D=9$ (right part). Only the seven lowest energy eigenstates are plotted with the numerals on the right labeling the eigenstates.

then continues to move along the second chain toward the end point 2i. The two stereo-irregular chains are now linked together.

If we increase the value of D to 5 and 7, similar results are shown at the left part and the right part, respectively, of Fig. 12. For large values of $R_0=5$ and 7, we found that all the states are localized. Therefore, there is no electron tunneling phenomena in these cases. The localization of the seven lowest energy states is shown in Fig. 13 for $R_0=5$ and in Fig. 14 for $R_0=7$.

It is clear by now that the existence of the bridge point introduces a large fluctuation in the moments for $R_0=3$. The fluctuation is gradually reduced as R_0 increases, as can be seen in Figs. 8–10.

The conclusion can be drawn as follows. If R_0 is not very large, the energy spectrum of two coupled stereo-irregular chains can be separated into a low-energy localized region, an intermediate-energy screening region, and a high-energy linking region.

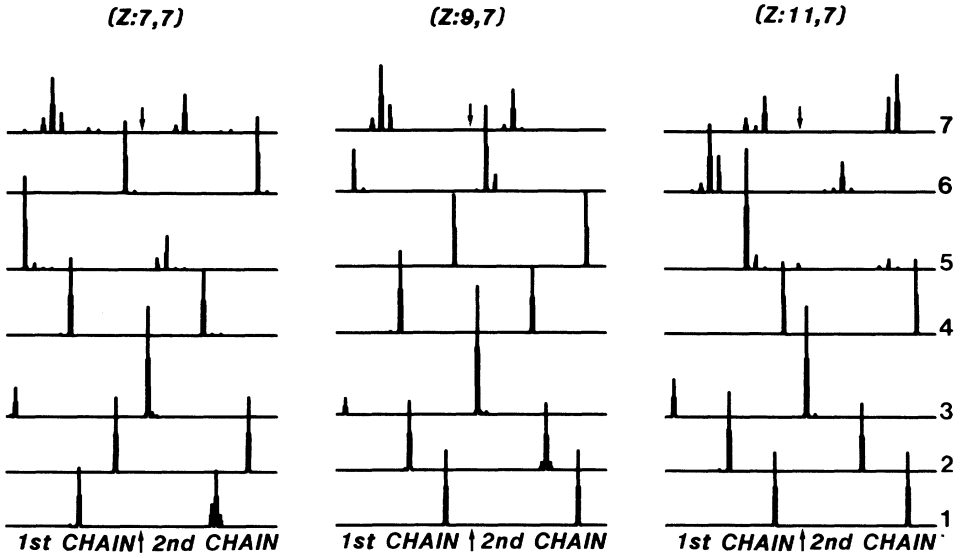

FIG. 14. The charge distribution along the coupled chains for $\sigma=\uparrow$, $R_0=7$, and $D=7$ (left part), $D=9$ (middle part), and $D=11$ (right part). Only the seven lowest energy eigenstates are plotted with the numerals on the right labeling the eigenstates.

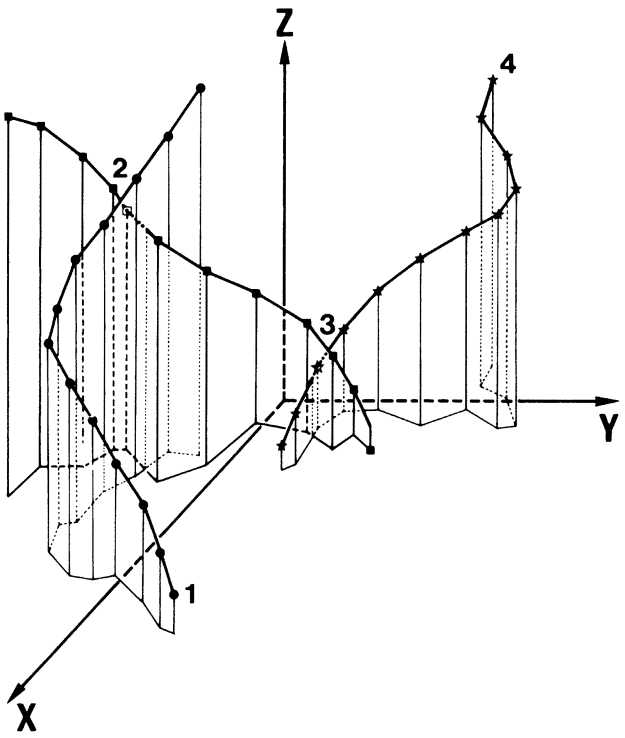

FIG. 15. Schematic plot of three interacting chains coupled at two bridge points.

VI. FINAL REMARK

We have discussed in Sec. II that in a system of intermingled stereo-irregular chains, each chain is crossed by other chains at a finite number of bridge points, provided the chain density is low and the angle θ_m is not too large. Figure 15 can be viewed as part of this system where one chain meets two other chains at two bridge points. Then, under suitable conditions there exist tunneling states linking these three chains from point 1 through points 2 and 3 to point 4. We then expect a finite dc conductivity. It is generally accepted that for many conducting polymers, the structure consists of many intermingled fibrils.

One weak point in the present calculation is the appearance of an energy gap between the two subspectra. Therefore, for one electron per atom, a gap separates the occupied and the empty parts of the density of states. The presence of this gap is most likely due to the use of the hydrogen 1*s* wave and the simplification of the system to only two interacting chains. If we use π orbitals to investigate a system of many interacting chains, the gap is expected to be removed. However, such a calculation probably will be beyond the capability of currently available computer.

Finally, we should point out that the chosen parameters do not represent simplified experimental properties. It is certainly not true that an experimental property is the complete geometric structure of a system. Our attempt is to include the structural randomness into a system of linear chains and demonstrate the role of the bridge points as the tunneling region, which was not suggested elsewhere. Of course, a more sophisticated solution on this problem requires the statistical-mechanics treatment on a system of randomly distributed bridge points connected by conducting segments.

[1]P. W. Anderson, Phys. Rev. 109, 1492 (1958).
[2]D. C. Herbert and R. Jones, J. Phys. C 4, 1145 (1971).
[3]W. H. Butler, Phys. Rev. B 8, 4499 (1973).
[4]B. J. Last and D. J. Thouless, J. Phys. C 7, 699 (1974).
[5]D. Weaire and A. R. Williams, J. Phys. C 9, L461 (1976).
[6]S. Yoshino and M. Okazaki, J. Phys. Soc. Jpn. 43, 415 (1977).
[7]J. C. Kimball, J. Phys. C 11, 1367 (1978).
[8]R. C. Albers and J. E. Gubernatis, Phys. Rev. B 17, 4487 (1978).
[9]K. Tsujino, M. Yamamoto, A. Tokunaga, and F. Yonezawa, Solid State Commun. 30, 531 (1979).
[10]P. M. Richards and R. L. Renken, Phys. Rev. B 21, 3740 (1980).
[11]R. Day and F. Martino, J. Phys. C 14, 4247 (1981).
[12]V. M. Koleshko and N. Yu. Trifonov, Phys. Status Solidi B 104, K105 (1981).
[13]F. Tanaka, Prog. Theor. Phys. 65, 751 (1981).
[14]W. Y. Ching and D. L. Huber, Phys. Rev. B 26, 5596 (1982).
[15]J. M. Andre, Adv. Quantum Chem. 12, 65 (1980).
[16]A. Karpfen and P. Schuster, Chem. Phys. Lett. 44, 459 (1976).
[17]R. A. Harris and L. M. Falicov, J. Chem. Phys. 51, 5034 (1969).
[18]M. Kertesz, Phys. Status Solidi B 69, K141 (1975).
[19]A. Karpfen, J. Phys. C 12, 3227 (1979).
[20]J. Delhalle, L. Piela, J.-L. Bredas, and J. M. Andre, Phys. Rev. B 22, 6254 (1980).
[21]G. Del Re, J. Ladik, and G. Biczo, Phys. Rev. 155, 997 (1967).
[22]J. M. Andre, J. Chem. Phys. 50, 1536 (1969).
[23]M. Kertesz, J. Koller, A. Azman, and S. Suhai, Phys. Lett. 55A, 107 (1975).
[24]C. Merkel and J. Ladik, Phys. Lett. 56A, 395 (1976).
[25]J. Ladik and M. Seel, Phys. Rev. B 13, 5338 (1976).
[26]R. Hoffman, J. Chem. Phys. 39, 1397 (1963).
[27]J. Delhalle, J. M. Andre, S. Delhalle, J. J. Pireaux, R. Caudano, and J. J. Verbist, J. Chem. Phys. 60, 595 (1974).

[28]M. Kertesz and G. Gondor, J. Phys. C 14, L851 (1981).
[29]A. Karffen, Chem. Phys. Lett. 64, 299 (1979).
[30]M. Seel, *Lecture Notes in Physics,* (Springer, Berlin 1979), Vol. 113, p. 271.
[31]W. L. McCubbin, Chem. Phys. Lett. 8, 507 (1971).
[32]J.-L. Calais, Ark. Fys. 28, 511 (1965).
[33]K.-F. Berggren and F. Martino, Phys. Rev. 184, 484 (1969).
[34]D. H. Kislow, J. M. McKelvey, C. F. Bender, and H. F. Schaefer, III, Phys. Rev. Lett. 32, 933 (1974).
[35]M. Kertesz, J. Koller, and A. Azman, Phys. Rev. B 14, 76 (1976).
[36]M. Kertesz, J. Koller, and A. Azman, Theor. Chem. Acta 41, 89 (1976).
[37]J. Delhalle and F. E. Harris, Theor. Chem. Acta 48, 127 (1978).
[38]R. S. Day, Phys. Lett. 85A, 405 (1981).
[39]S. Stafström, R. Riklund, and K. A. Chao, Phys. Rev. B 26, 4691 (1982).
[40]B. Horovitz, J. A. Krumhansl, and E. Domany, Phys. Rev. Lett. 38, 778 (1977).
[41]I. Batistić, G. Theodorou, and S. Barisić, J. Phys. C 14, 1905 (1981).
[42]R. J. Bell, P. Dean, and D. C. Hibbins-Butler, J. Phys. C 3, 2111 (1970).
[43]W. Y. Ching, Phys. Rev. Lett. 46, 607 (1981).
[44]S. Chandrasekhar, Astrophys. J. 100, 176 (1944).
[45]R. Riklund and K. A. Chao, Phys. Rev. B 26, 2168 (1982).